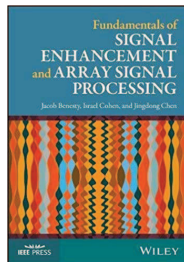


# Single-Channel Signal Enhancement in the Frequency Domain

J. Benesty, I. Cohen, and J. Chen,  
*Fundamentals of Signal Enhancement  
and Array Signal Processing*,  
Wiley-IEEE Press, 2017.



# Outline

- 1 Introduction
- 2 Signal Model and Problem Formulation
- 3 Noise Reduction with Gains
- 4 Performance Measures
- 5 Optimal Gains
- 6 Implementation with the Short-Time Fourier Transform

# Introduction

We study the signal enhancement problem in the frequency domain with a single sensor.

We show how to compromise between distortion of the desired signal and reduction of the additive noise.

The advantages of the frequency-domain technique are twofold.

First, it is very flexible in the sense that the observation signal at each frequency can be processed independently of the others.

Second, thanks to the fast Fourier transform, all algorithms can be implemented very efficiently.

# Signal Model and Problem Formulation

We recall that the observation signal in the time domain is

$$y(t) = x(t) + v(t), \quad (1)$$

where  $x(t)$  and  $v(t)$  are the desired and noise signals, respectively.

In the frequency domain, (1) can be written as

$$Y(f) = X(f) + V(f), \quad (2)$$

where  $Y(f)$ ,  $X(f)$ , and  $V(f)$  are the frequency-domain representations of  $y(t)$ ,  $x(t)$ , and  $v(t)$ , respectively, at the frequency index  $f$ .

Since the zero-mean signals  $X(f)$  and  $V(f)$  are assumed to be uncorrelated, the variance of  $Y(f)$  is

$$\begin{aligned}\phi_Y(f) &= E \left[ |Y(f)|^2 \right] \\ &= \phi_X(f) + \phi_V(f),\end{aligned}\tag{3}$$

where  $\phi_X(f) = E \left[ |X(f)|^2 \right]$  and  $\phi_V(f) = E \left[ |V(f)|^2 \right]$  are the variances of  $X(f)$  and  $V(f)$ , respectively.

The objective of single-channel noise reduction in the frequency domain is to find an estimate of  $X(f)$  from  $Y(f)$ .

## Noise Reduction with Gains

An estimate of  $X(f)$  can be obtained by multiplying  $Y(f)$  with a complex gain,  $H(f)$ , as illustrated in Fig. 1, i.e.,

$$\begin{aligned} Z(f) &= H(f)Y(f) \\ &= H(f) [X(f) + V(f)] \\ &= X_{\text{fd}}(f) + V_{\text{rn}}(f). \end{aligned} \tag{4}$$

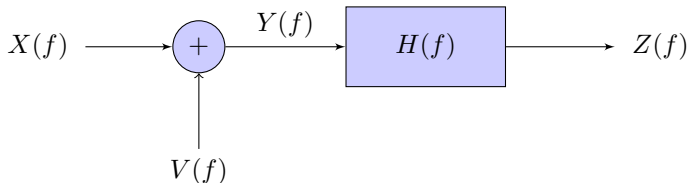


**Figure 1:** Block diagram of noise reduction with gains in the frequency domain.

The filtered desired signal is given by

$$X_{\text{fd}}(f) = H(f)X(f), \quad (5)$$

and the residual noise is given by

$$V_{\text{rn}}(f) = H(f)V(f). \quad (6)$$

The variance of  $Z(f)$  can be written as

$$\begin{aligned} \phi_Z(f) &= E \left[ |Z(f)|^2 \right] \\ &= |H(f)|^2 \phi_Y(f) \\ &= \phi_{X_{\text{fd}}}(f) + \phi_{V_{\text{rn}}}(f), \end{aligned} \quad (7)$$

where

$$\phi_{X_{\text{fd}}}(f) = |H(f)|^2 \phi_X(f) \quad (8)$$

is the variance of the filtered desired signal and

$$\phi_{V_{\text{rn}}}(f) = |H(f)|^2 \phi_V(f) \quad (9)$$

is the variance of the residual noise.

# Performance Measures

## Signal-to-Noise Ratio

We define the narrowband input SNR as

$$\text{iSNR}(f) = \frac{\phi_X(f)}{\phi_V(f)}. \quad (10)$$

The broadband input SNR is obtained by simply integrating over all frequencies the numerator and denominator of  $\text{iSNR}(f)$ .

We get

$$\text{iSNR} = \frac{\int_f \phi_X(f) df}{\int_f \phi_V(f) df}. \quad (11)$$

After noise reduction with the frequency-domain model given in (4), the narrowband output SNR can be written as

$$\text{oSNR}[H(f)] = \frac{\phi_{X_{\text{fd}}}(f)}{\phi_{V_{\text{rn}}}(f)} = \text{iSNR}(f). \quad (12)$$

It is important to observe that the narrowband output SNR is not influenced by  $H(f)$ .

We deduce that the broadband output SNR is

$$\text{oSNR}(H) = \frac{\int_f \phi_{X_{\text{fd}}}(f) df}{\int_f \phi_{V_{\text{rn}}}(f) df} = \frac{\int_f |H(f)|^2 \phi_X(f) df}{\int_f |H(f)|^2 \phi_V(f) df}. \quad (13)$$

It is essential to find the complex gains  $H(f)$  at all frequencies in such a way that  $\text{oSNR}(H) > \text{iSNR}$ .

# Noise Reduction Factor

We define the narrowband and broadband noise reduction factors as, respectively,

$$\xi_n [H(f)] = \frac{1}{|H(f)|^2} \quad (14)$$

and

$$\xi_n (H) = \frac{\int_f \phi_V(f) df}{\int_f |H(f)|^2 \phi_V(f) df}. \quad (15)$$

The larger the values of the noise reduction factors are, the more reduced the noise is.

## Desired-Signal Reduction Factor

In the same way, we define the narrowband and broadband desired-signal reduction factors as, respectively,

$$\xi_d [H(f)] = \frac{1}{|H(f)|^2} \quad (16)$$

and

$$\xi_d (H) = \frac{\int_f \phi_X(f) df}{\int_f |H(f)|^2 \phi_X(f) df}. \quad (17)$$

The larger the values of the desired-signal reduction factors are, the more distorted the desired signal is.

We always have

$$\frac{o\text{SNR}(H)}{i\text{SNR}} = \frac{\xi_n(H)}{\xi_d(H)}. \quad (18)$$

This means that the gain in SNR comes with the distortion of the desired and noise signals.

## Desired-Signal Distortion Index

Another way to quantify distortion is via the narrowband desired-signal distortion index:

$$v_d [H(f)] = \frac{E \left[ |H(f)X(f) - X(f)|^2 \right]}{\phi_X(f)} = |1 - H(f)|^2 \quad (19)$$

and the broadband desired-signal distortion index:

$$\begin{aligned} v_d (H) &= \frac{\int_f E \left[ |H(f)X(f) - X(f)|^2 \right] df}{\int_f \phi_X(f) df} \\ &= \frac{\int_f |1 - H(f)|^2 \phi_X(f) df}{\int_f \phi_X(f) df}. \end{aligned} \quad (20)$$

The desired-signal distortion index has a lower bound of 0 and an upper bound of 1 for optimal gains.

## Mean-Squared Error

We define the error signal between the estimated and desired signals at frequency  $f$  as

$$\begin{aligned}\mathcal{E}(f) &= Z(f) - X(f) \\ &= H(f)Y(f) - X(f).\end{aligned}\tag{21}$$

This error can also be put into the form:

$$\mathcal{E}(f) = \mathcal{E}_d(f) + \mathcal{E}_n(f),\tag{22}$$

where

$$\mathcal{E}_d(f) = [H(f) - 1] X(f)\tag{23}$$

is the desired-signal distortion due to the complex gain and

$$\mathcal{E}_n(f) = H(f)V(f)\tag{24}$$

represents the residual noise.

The narrowband MSE criterion is then

$$\begin{aligned} J[H(f)] &= E \left[ |\mathcal{E}(f)|^2 \right] \\ &= |1 - H(f)|^2 \phi_X(f) + |H(f)|^2 \phi_V(f). \end{aligned} \quad (25)$$

The narrowband MSE is also

$$\begin{aligned} J[H(f)] &= E \left[ |\mathcal{E}_d(f)|^2 \right] + E \left[ |\mathcal{E}_n(f)|^2 \right] \\ &= J_d[H(f)] + J_n[H(f)], \end{aligned} \quad (26)$$

where

$$J_d[H(f)] = \phi_X(f) v_d[H(f)] \quad (27)$$

and

$$J_n[H(f)] = \frac{\phi_V(f)}{\xi_n[H(f)]}. \quad (28)$$

We deduce that

$$J[H(f)] = \phi_V(f) \left\{ \text{iSNR}(f) \times v_d[H(f)] + \frac{1}{\xi_n[H(f)]} \right\} \quad (29)$$

and

$$\begin{aligned} \frac{J_d[H(f)]}{J_n[H(f)]} &= \text{iSNR}(f) \times \xi_n[H(f)] \times v_d[H(f)] \\ &= \text{oSNR}[H(f)] \times \xi_d[H(f)] \times v_d[H(f)], \end{aligned} \quad (30)$$

showing how the narrowband MSEs are related to the different narrowband performance measures.

The extension of the narrowband MSE to the broadband case is straightforward.

We define the broadband MSE criterion as

$$\begin{aligned}
 J(H) &= \int_f J[H(f)] df \\
 &= \int_f |1 - H(f)|^2 \phi_X(f) df + \int_f |H(f)|^2 \phi_V(f) df \\
 &= J_d(H) + J_n(H),
 \end{aligned} \tag{31}$$

where

$$J_d(H) = v_d(H) \int_f \phi_X(f) df \tag{32}$$

$$J_n(H) = \frac{\int_f \phi_V(f) df}{\xi_n(H)}. \tag{33}$$

# Optimal Gains

## Wiener Filter

Taking the gradient of  $J[H(f)]$  [eq. (25)] with respect to  $H^*(f)$  and equating the result to 0 lead to

$$-E\{Y^*(f)[X(f) - H_W(f)Y(f)]\} = 0. \quad (34)$$

Hence,

$$\phi_Y(f)H_W(f) = \phi_{XY}(f), \quad (35)$$

where

$$\begin{aligned} \phi_{XY}(f) &= E[X(f)Y^*(f)] \\ &= \phi_X(f) \end{aligned} \quad (36)$$

is the the cross-correlation between  $X(f)$  and  $Y(f)$ , which simplifies to the variance of  $X(f)$  in this particular model.

Therefore, the optimal Wiener gain can be put into the following forms:

$$\begin{aligned} H_W(f) &= \frac{\phi_X(f)}{\phi_Y(f)} \\ &= 1 - \frac{\phi_V(f)}{\phi_Y(f)} \\ &= \frac{i\text{SNR}(f)}{1 + i\text{SNR}(f)}. \end{aligned} \tag{37}$$

This gain is always real, positive, and smaller than one.

Another way to write the Wiener gain is with the magnitude squared coherence functions (MSCFs). Indeed, it is easy to see that

$$\begin{aligned} H_W(f) &= |\rho[X(f), Y(f)]|^2 \\ &= 1 - |\rho[V(f), Y(f)]|^2, \end{aligned} \tag{38}$$

where

$$\begin{aligned} |\rho[X(f), Y(f)]|^2 &= \frac{|E[X(f)Y^*(f)]|^2}{E[|X(f)|^2] E[|Y(f)|^2]} \\ &= \frac{|\phi_{XY}(f)|^2}{\phi_X(f)\phi_Y(f)} = \frac{i\text{SNR}(f)}{1 + i\text{SNR}(f)} \end{aligned} \quad (39)$$

is the MSCF between  $X(f)$  and  $Y(f)$ , and

$$\begin{aligned} |\rho[V(f), Y(f)]|^2 &= \frac{|\phi_{VY}(f)|^2}{\phi_V(f)\phi_Y(f)} \\ &= \frac{1}{1 + i\text{SNR}(f)} \end{aligned} \quad (40)$$

is the MSCF between  $V(f)$  and  $Y(f)$ .

When the level of the noise is high at frequency  $f$ ,  $|\rho[V(f), Y(f)]|^2 \approx 1$ , then  $H_W(f)$  is close to 0 since there is a large amount of noise that needs to be removed.

When the level of the noise is low at frequency  $f$ ,  $|\rho[V(f), Y(f)]|^2 \approx 0$ , then  $H_W(f)$  is close to 1 and this gain is not going to affect much the signals since there is little noise that needs to be removed.

Now, let us define the complex number<sup>1</sup>:

$$\begin{aligned}\varrho[X(f), V(f)] &= \rho[X(f), Y(f)] + j\rho[V(f), Y(f)] \\ &= \cos\theta(f) + j\sin\theta(f),\end{aligned}\tag{41}$$

where  $j = \sqrt{-1}$  is the imaginary unit and  $\theta(f)$  is the phase of  $\varrho[X(f), V(f)]$  whose modulus is equal to 1.

---

<sup>1</sup>Notice that both  $\rho[X(f), Y(f)]$  and  $\rho[V(f), Y(f)]$  are real numbers.

On the complex plane,  $\varrho[X(f), V(f)]$  is on the unit circle.

Since  $0 \leq \rho[X(f), Y(f)] \leq 1$  and  $0 \leq \rho[V(f), Y(f)] \leq 1$ , therefore  $0 \leq \theta(f) \leq \frac{\pi}{2}$ .

We can then rewrite the Wiener gain as a function of the angle  $\theta(f)$ , i.e.,

$$\begin{aligned} H_W(f) &= \cos^2 \theta(f) \\ &= 1 - \sin^2 \theta(f). \end{aligned} \tag{42}$$

Hence,

$$\lim_{\theta(f) \rightarrow 0} H_W(f) = 1, \tag{43}$$

$$\lim_{\theta(f) \rightarrow \frac{\pi}{2}} H_W(f) = 0. \tag{44}$$

The MMSE is obtained by replacing (37) in (25):

$$\begin{aligned} J[H_W(f)] &= \phi_X(f) - \frac{\phi_X^2(f)}{\phi_Y(f)} \\ &= \phi_V(f) - \frac{\phi_V^2(f)}{\phi_Y(f)}, \end{aligned} \tag{45}$$

which can be rewritten as

$$\begin{aligned} J[H_W(f)] &= \phi_X(f) \left\{ 1 - |\rho[X(f), Y(f)]|^2 \right\} \\ &= \phi_V(f) \left\{ 1 - |\rho[V(f), Y(f)]|^2 \right\} \\ &= H_W(f) \phi_V(f) \\ &= [1 - H_W(f)] \phi_X(f). \end{aligned} \tag{46}$$

We deduce all the narrowband performance measures with the Wiener gain:

$$\xi_n [H_W(f)] = \frac{1}{\cos^4 \theta(f)} \geq 1, \quad (47)$$

$$\xi_d [H_W(f)] = \frac{1}{\cos^4 \theta(f)} \geq 1, \quad (48)$$

$$v_d [H_W(f)] = \sin^4 \theta(f) \leq 1. \quad (49)$$

We recall that the narrowband output SNR is equal to the narrowband input SNR.

Figure 2 shows plots of the optimal Wiener gain,  $H_W(f)$ , the angle,  $\theta(f)$ , the narrowband noise reduction factor,  $\xi_n[H_W(f)]$ , and the narrowband desired-signal distortion index,  $v_d[H_W(f)]$ , as a function of the narrowband input SNR.

As the input SNR increases, the Wiener gain increases, since there is less noise to suppress.

As a result, both the noise reduction factor and the desired-signal distortion index decrease.

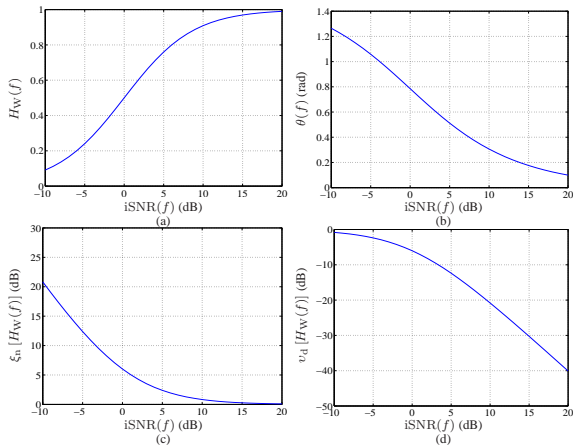


**Figure 2:** (a) The optimal Wiener gain, (b) the angle, (c) the narrowband noise reduction factor, and (d) the narrowband desired-signal distortion index as a function of the narrowband input SNR.

## Property

*With the optimal Wiener gain given in (37), the broadband output SNR is always greater than or equal to the broadband input SNR, i.e.,  $\text{oSNR}(H_W) \geq \text{iSNR}$ .*

**Proof.** The broadband MSCF, which is equivalent to the SPCC, between the two zero-mean random variables  $A(f)$  and  $B(f)$ , which

are the frequency-domain representations of the time-domain real signals  $a(t)$  and  $b(t)$ , is defined as

$$\begin{aligned}
 |\rho(A, B)|^2 &= \frac{\left| E \left[ \int_f A(f) B^*(f) df \right] \right|^2}{E \left[ \int_f |A(f)|^2 df \right] E \left[ \int_f |B(f)|^2 df \right]} \quad (50) \\
 &= \frac{\left| \int_f \phi_{AB}(f) df \right|^2}{\left[ \int_f \phi_A(f) df \right] \left[ \int_f \phi_B(f) df \right]} \\
 &= \frac{E^2[a(t)b(t)]}{\sigma_a^2 \sigma_b^2} \\
 &= \rho^2(a, b).
 \end{aligned}$$

Let us evaluate the broadband MSCF between  $Y(f)$  and  $Z_W(f) = H_W(f)Y(f)$ :

$$\begin{aligned}
 |\rho(Y, Z_W)|^2 &= \frac{\left[ \int_f H_W(f) \phi_Y(f) df \right]^2}{\left[ \int_f \phi_Y(f) df \right] \left[ \int_f H_W^2(f) \phi_Y(f) df \right]} \\
 &= \frac{\int_f \phi_X(f) df}{\int_f \phi_Y(f) df} \times \frac{\int_f \phi_X(f) df}{\int_f H_W(f) \phi_X(f) df} \\
 &= \frac{|\rho(X, Y)|^2}{|\rho(X, Z_W)|^2}.
 \end{aligned}$$

Therefore,

$$|\rho(X, Y)|^2 = |\rho(Y, Z_W)|^2 \times |\rho(X, Z_W)|^2 \leq |\rho(X, Z_W)|^2. \quad (51)$$

On the other hand, it can be shown that

$$|\rho(X, Y)|^2 = \frac{i\text{SNR}}{1 + i\text{SNR}}$$

and

$$|\rho(X, Z_W)|^2 \leq \frac{o\text{SNR}(H_W)}{1 + o\text{SNR}(H_W)}.$$

Substituting the two previous expressions into (51), we obtain

$$\frac{i\text{SNR}}{1 + i\text{SNR}} \leq \frac{o\text{SNR}(H_W)}{1 + o\text{SNR}(H_W)}.$$

As a result, we have  $o\text{SNR}(H_W) \geq i\text{SNR}$ .

## Example 1

Consider a desired signal,  $X(f)$ , with the variance:

$$\phi_X(f) = \begin{cases} \alpha, & |f| \leq \frac{1}{4} \\ 0, & \frac{1}{4} \leq |f| \leq \frac{1}{2} \end{cases},$$

that is corrupted with additive noise,  $V(f)$ , with the variance:

$$\phi_V(f) = \beta (1 - 2|f|), \quad -\frac{1}{2} \leq |f| \leq \frac{1}{2}.$$

The desired signal is uncorrelated with the noise, and needs to be recovered from the noisy observation,  $Y(f) = X(f) + V(f)$ .

The narrowband input SNR is

$$\begin{aligned} \text{iSNR}(f) &= \frac{\phi_X(f)}{\phi_V(f)} \\ &= \begin{cases} \frac{\alpha}{\beta} (1 - 2|f|)^{-1}, & |f| \leq \frac{1}{4} \\ 0, & \frac{1}{4} \leq |f| \leq \frac{1}{2} \end{cases} \end{aligned}$$

and the broadband input SNR is

$$\begin{aligned} \text{iSNR} &= \frac{\int_f \phi_X(f) df}{\int_f \phi_V(f) df} \\ &= \frac{\alpha}{\beta}. \end{aligned}$$

The optimal Wiener gain is given by

$$H_W(f) = \frac{i\text{SNR}(f)}{1 + i\text{SNR}(f)}$$

$$= \begin{cases} \frac{\alpha}{\beta} \left( \frac{\alpha}{\beta} + 1 - 2|f| \right)^{-1}, & |f| \leq \frac{1}{4} \\ 0, & \frac{1}{4} \leq |f| \leq \frac{1}{2} \end{cases}.$$

The broadband output SNR,  $\text{oSNR}(H_W)$ , is computed using (13), and the broadband gain in SNR is obtained by

$$\mathcal{G}(H_W) = \text{oSNR}(H_W) / i\text{SNR}.$$

Figure 3 shows plots of the broadband gain in SNR, the broadband MSE,  $J(H_W)$ , the broadband noise reduction factor,  $\xi_n(H_W)$ , and the broadband desired-signal reduction factor,  $\xi_d(H_W)$ , as a function of the broadband input SNR.

As the input SNR increases, less noise needs to be suppressed, and less distortion is introduced into the filtered desired signal.

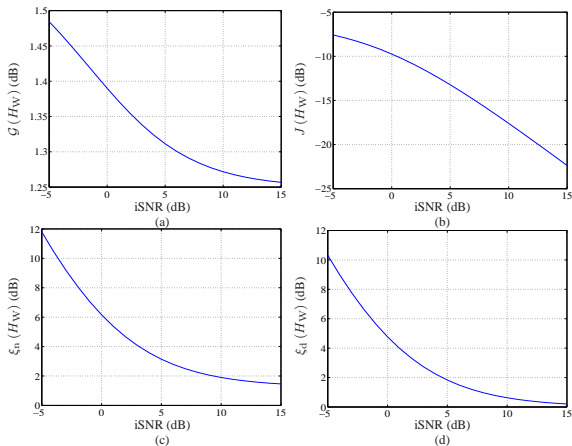


**Figure 3:** (a) The broadband gain in SNR, (b) the broadband MSE, (c) the broadband noise reduction factor, and (d) the broadband desired-signal reduction factor of the Wiener gain as a function of the broadband input SNR.

## Example 2

Suppose that the desired signal is a harmonic pulse of  $T$  samples:

$$x(t) = \begin{cases} A \sin(2\pi f_0 t + \phi), & 0 \leq t \leq T-1 \\ 0, & t < 0, t \geq T \end{cases},$$

with fixed amplitude  $A$  and frequency  $f_0$ , and random phase  $\phi$ , uniformly distributed on the interval from 0 to  $2\pi$ .

This signal needs to be recovered from the noisy observation,  $y(t) = x(t) + v(t)$ , where  $v(t)$  is additive white Gaussian noise, i.e.,  $v(t) \sim \mathcal{N}(0, \sigma_v^2)$ , that is uncorrelated with  $x(t)$ .

The frequency-domain representation of the desired signal is given by

$$\begin{aligned} X(f) &= \sum_{t=-\infty}^{\infty} x(t) e^{j2\pi f t} \\ &= \sum_{t=0}^{T-1} A \sin(2\pi f_0 t + \phi) e^{j2\pi f t} \\ &= \frac{A}{2j} e^{j\phi + j\pi(f+f_0)(T-1)} D_T[\pi(f+f_0)] + \\ &\quad \frac{A}{2j} e^{-j\phi + j\pi(f-f_0)(T-1)} D_T[\pi(f-f_0)], \end{aligned}$$

where the function  $D_T(x)$  is the Dirichlet kernel defined as

$$D_T(x) = \frac{\sin(Tx)}{\sin(x)}.$$

Hence, the variance of  $X(f)$  is

$$\phi_X(f) = \frac{A^2}{4} D_T^2 [\pi (f + f_0)] + \frac{A^2}{4} D_T^2 [\pi (f - f_0)].$$

The frequency-domain representation of the noise signal is

$$V(f) = \sum_{t=0}^{T-1} v(t) e^{j2\pi f t}.$$

Hence, the variance of  $V(f)$  is  $\phi_V(f) = T\sigma_v^2$ . The narrowband input SNR is

$$\begin{aligned} \text{iSNR}(f) &= \frac{\phi_X(f)}{\phi_V(f)} \\ &= \frac{A^2}{4T\sigma_v^2} D_T^2 [\pi (f + f_0)] + \frac{A^2}{4T\sigma_v^2} D_T^2 [\pi (f - f_0)] \end{aligned}$$

and the broadband input SNR is

$$\begin{aligned} \text{iSNR} &= \frac{\int_f \phi_X(f) df}{\int_f \phi_V(f) df} \\ &= \frac{\sum_t E \left[ |x(t)|^2 \right]}{\sum_t E \left[ |v(t)|^2 \right]} \\ &= \frac{A^2}{2\sigma_v^2}, \end{aligned}$$

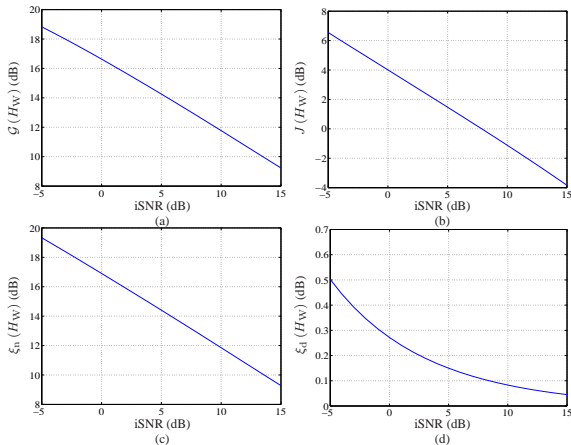
where we have used Parseval's identity.

The optimal Wiener gain is obtained from (37).

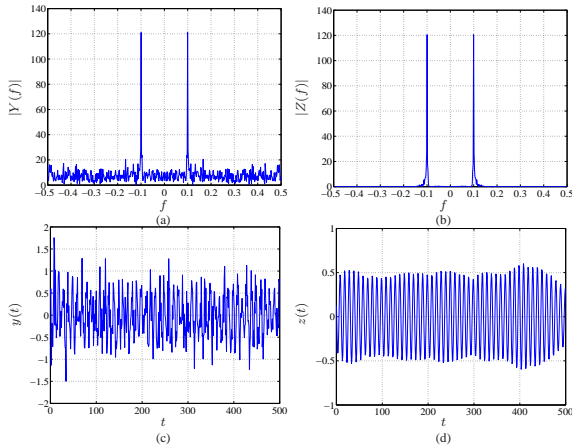
To demonstrate the performance of the Wiener gain, we choose  $A = 0.5$ ,  $f_0 = 0.1$ , and  $T = 500$ .

Figure 4 shows plots of the broadband gain in SNR, the broadband MSE,  $J(H_W)$ , the broadband noise reduction factor,  $\xi_n(H_W)$ , and the broadband desired-signal reduction factor,  $\xi_d(H_W)$ , as a function of the broadband input SNR.

Figure 5 shows a realization of the noise corrupted and filtered sinusoidal signals for  $i\text{SNR} = 0$  dB.



**Figure 4:** (a) The broadband gain in SNR, (b) the broadband MSE, (c) the broadband noise reduction factor, and (d) the broadband desired-signal reduction factor of the Wiener gain as a function of the broadband input SNR.



**Figure 5:** Example of noise corrupted and Wiener filtered sinusoidal signals for  $\text{iSNR} = 0$  dB. (a) Magnitude of frequency-domain observation signal,  $|Y(f)|$ , (b) magnitude of frequency-domain estimated signal,  $|Z(f)|$ , (c) time-domain observation signal,  $y(t)$ , and (d) time-domain estimated signal,  $z(t)$ .

## Tradeoff Gain

An important gain can be designed by minimizing the desired-signal distortion-based MSE with the constraint that the noise reduction-based MSE is equal to a positive number smaller than the level of the original noise.

This optimization problem can be translated mathematically as

$$\min_{H(f)} J_d [H(f)] \quad \text{subject to} \quad J_n [H(f)] = \aleph \phi_V(f), \quad (52)$$

where

$$J_d [H(f)] = |1 - H(f)|^2 \phi_X(f), \quad (53)$$

$$J_n [H(f)] = |H(f)|^2 \phi_V(f), \quad (54)$$

and  $0 < \aleph < 1$  to ensure that we have some noise reduction at frequency  $f$ .

If we use a Lagrange multiplier,  $\mu(f) \geq 0$ , to adjoin the constraint to the cost function, we easily find the tradeoff gain:

$$\begin{aligned}
 H_{T,\mu}(f) &= \frac{\phi_X(f)}{\phi_X(f) + \mu(f)\phi_V(f)} \\
 &= \frac{\phi_Y(f) - \phi_V(f)}{\phi_Y(f) + [\mu(f) - 1]\phi_V(f)} \\
 &= \frac{i\text{SNR}(f)}{\mu(f) + i\text{SNR}(f)}.
 \end{aligned} \tag{55}$$

This gain can be seen as a Wiener gain with an adjustable input noise level  $\mu(f)\phi_V(f)$ .

Obviously, the particular case of  $\mu(f) = 1$  corresponds to the Wiener gain.

We can also find the optimal  $\mu(f)$  corresponding to a given value of  $\aleph$ .

Substituting  $H_{T,\mu}(f)$  from (55) into the constraint in (52), we get

$$\begin{aligned} J_n [H_{T,\mu}(f)] &= |H_{T,\mu}(f)|^2 \phi_V(f) \\ &= \aleph \phi_V(f). \end{aligned} \quad (56)$$

From the previous expression, we easily find that

$$\mu(f) = \text{iSNR}(f) \frac{1 - \sqrt{\aleph}}{\sqrt{\aleph}} \quad (57)$$

and the tradeoff simplifies to a constant gain:

$$H_{T,\aleph} = \sqrt{\aleph}. \quad (58)$$

In the rest, we assume that  $\mu(f)$  is a constant, so it does not depend on frequency and we can drop the variable  $f$ . Usually, the value of  $\mu$  is given by design.

The MSCF between the two signals  $X(f)$  and  $X(f) + \sqrt{\mu}V(f)$  at frequency  $f$  is

$$|\rho[X(f), X(f) + \sqrt{\mu}V(f)]|^2 = \frac{\text{iSNR}(f)}{\mu + \text{iSNR}(f)}. \quad (59)$$

The MSCF between the two signals  $V(f)$  and  $X(f) + \sqrt{\mu}V(f)$  at frequency  $f$  is

$$|\rho[V(f), X(f) + \sqrt{\mu}V(f)]|^2 = \frac{\mu}{\mu + \text{iSNR}(f)}. \quad (60)$$

Therefore, we can write the tradeoff gain as a function of these two MSCFs:

$$\begin{aligned} H_{T,\mu}(f) &= |\rho[X(f), X(f) + \sqrt{\mu}V(f)]|^2 \\ &= 1 - |\rho[V(f), X(f) + \sqrt{\mu}V(f)]|^2. \end{aligned} \quad (61)$$

Now, let us define the complex number:

$$\begin{aligned}\varrho_{\mu} [X(f), V(f)] &= \rho [X(f), X(f) + \sqrt{\mu}V(f)] \\ &\quad + j\rho [V(f), X(f) + \sqrt{\mu}V(f)] \\ &= \cos \theta_{\mu}(f) + j \sin \theta_{\mu}(f),\end{aligned}\tag{62}$$

where  $\theta_{\mu}(f)$  is the phase of  $\varrho_{\mu} [X(f), V(f)]$  whose modulus is equal to 1.

Since  $0 \leq \rho [X(f), X(f) + \sqrt{\mu}V(f)] \leq 1$  and  $0 \leq \rho [V(f), X(f) + \sqrt{\mu}V(f)] \leq 1$ , therefore  $0 \leq \theta_{\mu}(f) \leq \frac{\pi}{2}$ .

We can then rewrite the tradeoff gain as a function of the angle  $\theta_{\mu}(f)$ :

$$\begin{aligned}H_{T,\mu}(f) &= \cos^2 \theta_{\mu}(f) \\ &= 1 - \sin^2 \theta_{\mu}(f).\end{aligned}\tag{63}$$

We deduce all the narrowband performance measures with the tradeoff gain:

$$\text{oSNR} [H_{T,\mu}(f)] = \text{iSNR}(f), \quad (64)$$

$$\xi_n [H_{T,\mu}(f)] = \frac{1}{\cos^4 \theta_\mu(f)} \geq 1, \quad (65)$$

$$\xi_d [H_{T,\mu}(f)] = \frac{1}{\cos^4 \theta_\mu(f)} \geq 1, \quad (66)$$

$$v_d [H_{T,\mu}(f)] = \sin^4 \theta_\mu(f) \leq 1. \quad (67)$$

Figure 6 shows plots of the tradedoff gain,  $H_{T,\mu}(f)$ , the angle,  $\theta_\mu(f)$ , the narrowband noise reduction factor,  $\xi_n[H_{T,\mu}(f)]$ , and the narrowband desired-signal distortion index,  $v_d[H_{T,\mu}(f)]$ , as a function of the narrowband input SNR for different values of  $\mu$ .

For a given input SNR, higher value of  $\mu$  yields lower tradedoff gain.

Hence, both the noise reduction factor and the desired-signal distortion index monotonically increase as a function of  $\mu$ .

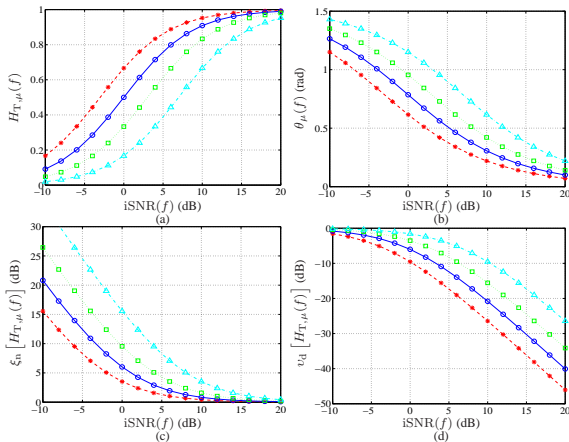


**Figure 6:** (a) The tradedoff gain, (b) the angle, (c) the narrowband noise reduction factor, and (d) the narrowband desired-signal distortion index for different values of  $\mu$ :  $\mu = 0.5$  (dashed line with asterisks),  $\mu = 1$  (solid line with circles),  $\mu = 2$  (dotted line with squares), and  $\mu = 5$  (dash-dot line with triangles).

## Property

*With the tradeoff gain given in (55), the broadband output SNR is always greater than or equal to the broadband input SNR, i.e.,*  
 $\text{oSNR}(H_{T,\mu}) \geq \text{iSNR}, \forall \mu \geq 0.$

**Proof.** The broadband MSCF between the two variables  $X(f)$  and  $X(f) + \sqrt{\mu}V(f)$  is

$$\begin{aligned} |\rho(X, X + \sqrt{\mu}V)|^2 &= \frac{\left[ \int_f \phi_X(f) df \right]^2}{\left[ \int_f \phi_X(f) df \right] \left[ \int_f \phi_X(f) df + \mu \int_f \phi_V(f) df \right]} \\ &= \frac{\text{iSNR}}{\mu + \text{iSNR}}. \end{aligned}$$

The broadband MSCF between the two variables  $X(f)$  and  $H_{T,\mu}(f)X(f) + \sqrt{\mu}H_{T,\mu}(f)V(f)$  is

$$\begin{aligned}
 |\rho(X, H_{T,\mu}X + \sqrt{\mu}H_{T,\mu}V)|^2 &= \frac{\left[ \int_f H_{T,\mu}(f) \phi_X(f) df \right]^2}{\left[ \int_f \phi_X(f) df \right] \left[ \int_f H_{T,\mu}^2(f) \phi_X(f) df + \mu \int_f H_{T,\mu}^2(f) \phi_V(f) df \right]} \\
 &= \frac{\int_f H_{T,\mu}(f) \phi_X(f) df}{\int_f \phi_X(f) df}.
 \end{aligned}$$

Another way to write the same broadband MSCF is the following:

$$\begin{aligned}
 |\rho(X, H_{T,\mu}X + \sqrt{\mu}H_{T,\mu}V)|^2 &= \frac{\left[\int_f H_{T,\mu}(f)\phi_X(f)df\right]^2}{\left[\int_f \phi_X(f)df\right] \left[\int_f H_{T,\mu}^2(f)\phi_X(f)df\right]} \times \\
 &\quad \frac{\text{oSNR}(H_{T,\mu})}{\mu + \text{oSNR}(H_{T,\mu})} \\
 &= |\rho(X, H_{T,\mu}X)|^2 \times \\
 &\quad |\rho(H_{T,\mu}X, H_{T,\mu}X + \sqrt{\mu}H_{T,\mu}V)|^2 \\
 &\leq \frac{\text{oSNR}(H_{T,\mu})}{\mu + \text{oSNR}(H_{T,\mu})}.
 \end{aligned}$$

Now, let us evaluate the broadband MSCF between the two variables  $X(f) + \sqrt{\mu}V(f)$  and  $H_{T,\mu}(f)X(f) + \sqrt{\mu}H_{T,\mu}(f)V(f)$ :

$$\begin{aligned}
 |\rho(X + \sqrt{\mu}V, H_{T,\mu}X + \sqrt{\mu}H_{T,\mu}V)|^2 &= \frac{\int_f \phi_X(f)df}{\int_f \phi_X(f)df + \mu \int_f \phi_V(f)df} \times \\
 &\quad \frac{\int_f \phi_X(f)df}{\int_f H_{T,\mu}(f)\phi_X(f)df} \\
 &= \frac{|\rho(X, X + \sqrt{\mu}V)|^2}{|\rho(X, H_{T,\mu}X + \sqrt{\mu}H_{T,\mu}V)|^2}.
 \end{aligned}$$

Therefore,

$$\begin{aligned}
 |\rho(X, X + \sqrt{\mu}V)|^2 &= \frac{\text{iSNR}}{\mu + \text{iSNR}} \\
 &= |\rho(X + \sqrt{\mu}V, H_{T,\mu}X + \sqrt{\mu}H_{T,\mu}V)|^2 \times \\
 &\quad |\rho(X, H_{T,\mu}X + \sqrt{\mu}H_{T,\mu}V)|^2 \\
 &\leq |\rho(X, H_{T,\mu}X + \sqrt{\mu}H_{T,\mu}V)|^2 \\
 &\leq \frac{\text{oSNR}(H_{T,\mu})}{\mu + \text{oSNR}(H_{T,\mu})}.
 \end{aligned}$$

As a result, we have

$$\text{oSNR}(H_{T,\mu}) \geq \text{iSNR}.$$



## Example 3

Returning to Example 1, Fig. 7 shows plots of the broadband gain in SNR,  $\mathcal{G}(H_{T,\mu})$ , the broadband MSE,  $J(H_{T,\mu})$ , the broadband noise reduction factor,  $\xi_n(H_{T,\mu})$ , and the broadband desired-signal reduction factor,  $\xi_d(H_{T,\mu})$ , as a function of the broadband input SNR for different values of  $\mu$ .

For a given broadband input SNR, the higher is the value of  $\mu$ , the higher are the broadband SNR gain and noise reduction, but at the expense of higher broadband desired-signal reduction.

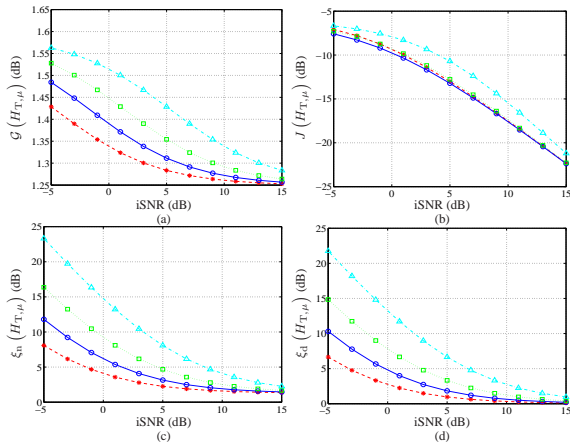


**Figure 7:** The broadband (a) gain in SNR, (b) MSE, (c) noise reduction factor, and (d) desired-signal reduction factor of the tradeoff gain for different values of  $\mu$ :  $\mu = 0.5$  (dashed line with asterisks),  $\mu = 1$  (solid line with circles),  $\mu = 2$  (dotted line with squares), and  $\mu = 5$  (dash-dot line with triangles).

# Parametric Wiener Gain

Some applications may need aggressive noise reduction while others may require little desired-signal distortion (and so less aggressive noise reduction).

An easy way to control the compromise between noise reduction and desired-signal distortion is via the parametric Wiener gain:

$$H_{\mu_1, \mu_2}(f) = [1 - \sin^{\mu_1} \theta(f)]^{\mu_2}, \quad (68)$$

where  $\mu_1$  and  $\mu_2$  are two positive parameters that allow the control of this compromise.

For  $(\mu_1, \mu_2) = (2, 1)$ , we get the Wiener gain developed previously.

Taking  $(\mu_1, \mu_2) = (2, 1/2)$ , leads to

$$\begin{aligned} H_{\text{pow}}(f) &= \sqrt{1 - \sin^2 \theta(f)} \\ &= \cos \theta(f), \end{aligned} \tag{69}$$

which is the power subtraction method studied in [2], [3], [4], [5], [6].

The pair  $(\mu_1, \mu_2) = (1, 1)$  gives the magnitude subtraction method [7], [8], [9], [10], [11]:

$$\begin{aligned} H_{\text{mag}}(f) &= 1 - \sin \theta(f) \\ &= 1 - \sqrt{1 - \cos^2 \theta(f)}. \end{aligned} \tag{70}$$

We can verify that the narrowband noise reduction factors for the power subtraction and magnitude subtraction methods are

$$\xi_n [H_{\text{pow}}(f)] = \frac{1}{\cos^2 \theta(f)}, \quad (71)$$

$$\xi_n [H_{\text{mag}}(f)] = \frac{1}{[1 - \sin \theta(f)]^2}, \quad (72)$$

and the corresponding narrowband desired-signal distortion indices are

$$v_d [H_{\text{pow}}(f)] = [1 - \cos \theta(f)]^2, \quad (73)$$

$$v_d [H_{\text{mag}}(f)] = \sin^2 \theta(f). \quad (74)$$

We can also easily check that

$$\xi_n [H_{\text{mag}}(f)] \geq \xi_n [H_W(f)] \geq \xi_n [H_{\text{pow}}(f)] , \quad (75)$$

$$v_d [H_{\text{pow}}(f)] \leq v_d [H_W(f)] \leq v_d [H_{\text{mag}}(f)] . \quad (76)$$

These inequalities are very important from a practical point of view.

They show that, among the three methods, the magnitude subtraction is the most aggressive one as far as noise reduction is concerned, a very well-known fact in the literature [12] but, at the same time, it is the one that will likely distort most the desired signal.

The smoothest approach is the power subtraction while the Wiener gain is between the two others in terms of desired-signal distortion and noise reduction.

Figure 8 shows plots of the parametric Wiener gain,  $H_{\mu_1, \mu_2}(f)$ , the narrowband noise reduction factor,  $\xi_n [H_{\mu_1, \mu_2}(f)]$ , and the narrowband desired-signal distortion index,  $v_d [H_{\mu_1, \mu_2}(f)]$ , as a function of the narrowband input SNR for different values of the pair  $(\mu_1, \mu_2)$ .

For a given input SNR,  $H_W(f)$  is larger than  $H_{\text{mag}}(f)$  and smaller than  $H_{\text{pow}}(f)$ .

Hence, the magnitude subtraction method is associated with higher noise reduction and desired-signal distortion than the Wiener method, while the power subtraction method is associated with less noise reduction and desired-signal distortion than the Wiener method.

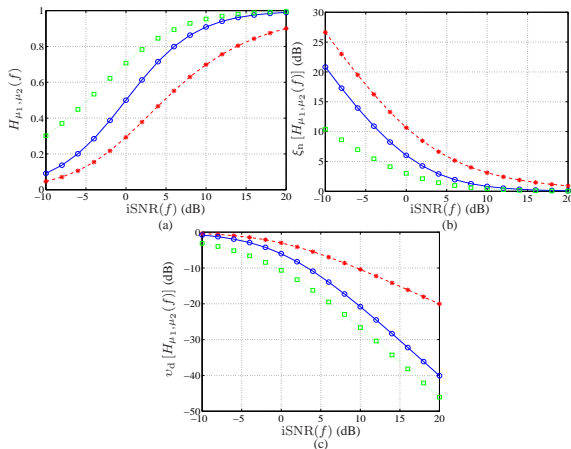


**Figure 8:** (a) The parametric Wiener gain, (b) noise reduction factor, and (c) desired-signal distortion index for: Magnitude subtraction with  $(\mu_1, \mu_2) = (1, 1)$  (dashed line with asterisks), Wiener gain with  $(\mu_1, \mu_2) = (2, 1)$  (solid line with circles), and power subtraction with  $(\mu_1, \mu_2) = (2, 1/2)$ .

## Example 4

Returning to Example 1, Fig. 9 shows plots of the broadband gain in SNR,  $\mathcal{G}(H_{\mu_1, \mu_2})$ , the broadband MSE,  $J(H_{\mu_1, \mu_2})$ , the broadband noise reduction factor,  $\xi_n(H_{\mu_1, \mu_2})$ , and the broadband desired-signal reduction factor,  $\xi_d(H_{\mu_1, \mu_2})$ , as a function of the broadband input SNR for different values of  $(\mu_1, \mu_2)$ .

For a given broadband input SNR, the magnitude subtraction method is associated with higher broadband SNR gain and noise reduction than the Wiener method, but at the expense of higher broadband desired-signal reduction.

On the other hand, the power subtraction method is associated with lower broadband desired-signal reduction than the Wiener method, but at the expense of lower broadband SNR gain and noise reduction.

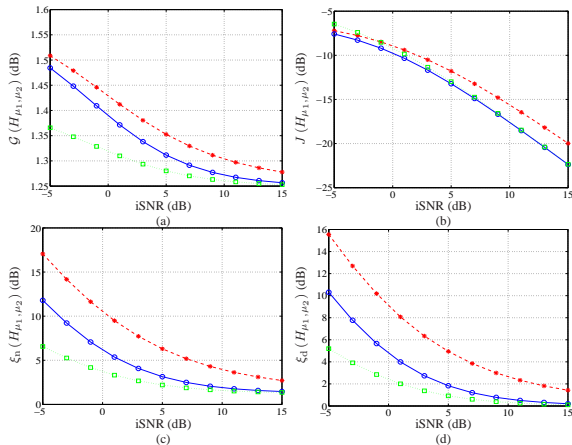


**Figure 9:** The broadband (a) gain in SNR, (b) MSE, (c) noise reduction factor, and (d) desired-signal reduction factor of the parametric Wiener gain for: Magnitude subtraction (dashed line with asterisks), Wiener gain (solid line with circles), and power subtraction (dotted line with squares).

Table 1 summarizes the optimal gains studied in this section.

**Table 1:** Optimal gains for single-channel signal enhancement in the frequency domain.

Wiener:	$H_W(f) = \frac{i\text{SNR}(f)}{1 + i\text{SNR}(f)}$
Tradeoff:	$H_{T,\mu}(f) = \frac{i\text{SNR}(f)}{\mu + i\text{SNR}(f)}, \mu \geq 0$
Param. Wiener:	$H_{\mu_1,\mu_2}(f) = [1 - \sin^{\mu_1} \theta(f)]^{\mu_2}, \mu_1, \mu_2 \geq 0$

# Implementation with the Short-Time Fourier Transform

In this section, we show how to implement the different gains in the short-time Fourier transform (STFT) domain.

The signal model given in (1) can be put into a vector form by considering the  $L$  most recent successive time samples, i.e.,

$$\mathbf{y}(t) = \mathbf{x}(t) + \mathbf{v}(t), \quad (77)$$

where

$$\mathbf{y}(t) = \begin{bmatrix} y(t) & y(t-1) & \cdots & y(t-L+1) \end{bmatrix}^T \quad (78)$$

is a vector of length  $L$ , and  $\mathbf{x}(t)$  and  $\mathbf{v}(t)$  are defined in a similar way to  $\mathbf{y}(t)$  from (78).

A short-time segment of the measured signal [i.e.,  $y(t)$ ], is multiplied with an analysis window of length  $L$ :

$$\mathbf{g} = \begin{bmatrix} g(0) & g(1) & \cdots & g(L-1) \end{bmatrix}^T \quad (79)$$

and transformed into the frequency domain by using the discrete Fourier transform (DFT). Let  $\mathbf{W}$  denote the DFT matrix of size  $L \times L$ , with

$$[\mathbf{W}]_{i,j} = \exp\left(-\frac{j2\pi ij}{L}\right), \quad i, j = 0, \dots, L-1. \quad (80)$$

Then, the STFT representation of the measured signal is defined as [16]

$$\mathbf{Y}(t) = \mathbf{W} \text{diag}(\mathbf{g}) \mathbf{y}(t), \quad (81)$$

where

$$\mathbf{Y}(t) = \begin{bmatrix} Y(t, 0) & Y(t, 1) & \cdots & Y(t, L-1) \end{bmatrix}^T. \quad (82)$$

In practice, the STFT representation is decimated in time by a factor  $R$  ( $1 \leq R \leq L$ ) [17]:

$$\begin{aligned} \mathbf{Y}(rR) &= \mathbf{Y}(t) \big|_{t=rR} \\ &= \begin{bmatrix} Y(rR, 0) & Y(rR, 1) & \cdots & Y(rR, L-1) \end{bmatrix}^T, \quad r \in \mathbb{Z}. \end{aligned} \quad (83)$$

Figure 10 shows the STFT representation of the measured signal.

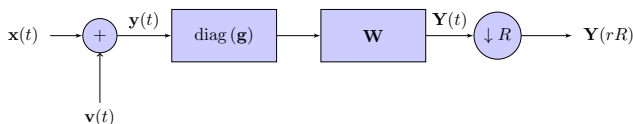


Figure 10: STFT representation of the measured signal.

Therefore, in the STFT domain, (1) can be written as

$$Y(rR, k) = X(rR, k) + V(rR, k), \quad (84)$$

where  $k = 0, \dots, L - 1$  denotes the frequency index, and  $X(rR, k)$  and  $V(rR, k)$  are the STFT representations of  $x(t)$  and  $v(t)$ , respectively.

Since the zero-mean signals  $X(rR, k)$  and  $V(rR, k)$  are assumed to be uncorrelated, the variance of  $Y(rR, k)$  is

$$\begin{aligned} \phi_Y(rR, k) &= E \left[ |Y(rR, k)|^2 \right] \\ &= \phi_X(rR, k) + \phi_V(rR, k), \end{aligned} \quad (85)$$

where  $\phi_X(rR, k) = E \left[ |X(rR, k)|^2 \right]$  and  $\phi_V(rR, k) = E \left[ |V(rR, k)|^2 \right]$  are the variances of  $X(rR, k)$  and  $V(rR, k)$ , respectively.

An estimate of  $X(rR, k)$  can be obtained by multiplying  $Y(rR, k)$  with a gain  $H(rR, k)$ , as illustrated in Fig. 11

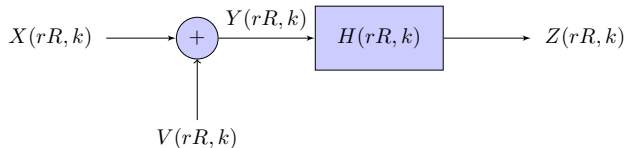


**Figure 11:** Block diagram of noise reduction in the STFT domain.

That is,

$$\begin{aligned} Z(rR, k) &= H(rR, k)Y(rR, k) \\ &= H(rR, k) [X(rR, k) + V(rR, k)] \\ &= X_{\text{fd}}(rR, k) + V_{\text{rn}}(rR, k), \end{aligned} \tag{86}$$

where  $Z(rR, k)$  is the STFT representation of the signal  $z(t)$ ,

$$X_{\text{fd}}(rR, k) = H(rR, k)X(rR, k) \tag{87}$$

is the filtered desired signal, and

$$V_{\text{rn}}(rR, k) = H(rR, k)V(rR, k) \tag{88}$$

is the residual noise.

A short-time segment of  $z(t)$  can be reconstructed in the time domain by applying the inverse DFT to the vector:

$$\mathbf{Z}(rR) = \begin{bmatrix} Z(rR, 0) & Z(rR, 1) & \cdots & Z(rR, L-1) \end{bmatrix}^T \quad (89)$$

and multiplying the result with a synthesis window of length  $L$ :

$$\tilde{\mathbf{g}} = \begin{bmatrix} \tilde{g}(0) & \tilde{g}(1) & \cdots & \tilde{g}(L-1) \end{bmatrix}^T. \quad (90)$$

That is,

$$\mathbf{z}(rR) = \text{diag}(\tilde{\mathbf{g}}) \mathbf{W}^H \mathbf{Z}(rR), \quad (91)$$

where the superscript  $^H$  denotes conjugate-transpose of a vector or a matrix.

The estimate  $z(t)$  of the desired signal can be reconstructed in the time domain by the overlap-add (OLA) method [18], i.e., summing the values at time  $t$  of all the short-time segments that overlap at time  $t$ :

$$z(t) = \sum_r \mathbf{i}_{rR-t+1}^T \mathbf{z}(rR), \quad (92)$$

where  $\mathbf{i}_i$  ( $1 \leq i \leq L$ ) is the  $i$ th column of  $\mathbf{I}_L$  and the summation is over integer values of  $r$  in the range  $\frac{t}{R} \leq r \leq \frac{t+L-1}{R}$ .

The inverse STFT is illustrated in Fig. 12.

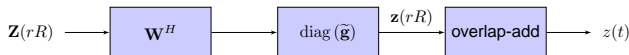


Figure 12: Block diagram of the inverse STFT.

The synthesis window  $\tilde{g}$  must satisfy a condition for exact reconstruction of  $x(t)$  when  $H(rR, k) = 1$  and  $V(rR, k) = 0$  for all  $(r, k)$  [17].

Specifically, from (81) we have

$$\mathbf{X}(rR) = \mathbf{W} \text{diag}(\mathbf{g}) \mathbf{x}(rR). \quad (93)$$

For exact reconstruction of  $z(t) = x(t)$  using (91) and (92), we require

$$x(t) = \sum_r \mathbf{i}_{rR-t+1}^T \text{diag}(\tilde{\mathbf{g}}) \mathbf{W}^H \mathbf{X}(rR). \quad (94)$$

Substituting (93) into (94), we get

$$x(t) = \sum_r \mathbf{i}_{rR-t+1}^T \text{diag}(\tilde{\mathbf{g}}) \text{diag}(\mathbf{g}) \mathbf{x}(rR), \quad (95)$$

for all signals  $x(t)$  and for all  $t$ .

Therefore, the condition for exact reconstruction is

$$\sum_r \tilde{g}(\ell + rR)g(\ell + rR) = 1, \forall \ell \in \{0, \dots, R-1\}. \quad (96)$$

## Property

*For a given analysis window  $g$  of length  $L > R$ , there are infinite solutions  $\tilde{g}$  that satisfy (96). A synthesis window of a minimal norm that satisfies (96) is given by [17]*

$$\tilde{g}(\ell) = \frac{g(\ell)}{\sum_r g^2(\ell + rR)}, \quad \ell = 0, \dots, L-1. \quad (97)$$

**Proof.** Define

$$\mathbf{g}_\ell = \begin{bmatrix} \cdots & g(\ell - R) & g(\ell) & g(\ell + R) & \cdots \end{bmatrix}^T, \\ \tilde{\mathbf{g}}_\ell = \begin{bmatrix} \cdots & \tilde{g}(\ell - R) & \tilde{g}(\ell) & \tilde{g}(\ell + R) & \cdots \end{bmatrix}^T.$$

Then condition (96) can be written as

$$\mathbf{g}_\ell^T \tilde{\mathbf{g}}_\ell = 1, \quad \forall \ell \in \{0, \dots, R-1\}. \quad (98)$$



The broadband input SNR is obtained by summing over all time-frequency indices the numerator and denominator of  $i\text{SNR}(rR, k)$ .

We get

$$i\text{SNR} = \frac{\sum_{r,k} \phi_X(rR, k)}{\sum_{r,k} \phi_V(rR, k)}. \quad (101)$$

Similarly, the broadband output SNR is

$$\begin{aligned} o\text{SNR}(H) &= \frac{\sum_{r,k} \phi_{X_{fd}}(rR, k)}{\sum_{r,k} \phi_{V_{rn}}(rR, k)} \\ &= \frac{\sum_{r,k} |H(rR, k)|^2 \phi_X(rR, k)}{\sum_{r,k} |H(rR, k)|^2 \phi_V(rR, k)}, \end{aligned} \quad (102)$$

the broadband noise reduction and desired-signal reduction factors are, respectively,

$$\xi_n(H) = \frac{\sum_{r,k} \phi_V(rR, k)}{\sum_{r,k} |H(rR, k)|^2 \phi_V(rR, k)}, \quad (103)$$

$$\xi_d(H) = \frac{\sum_{r,k} \phi_X(rR, k)}{\sum_{r,k} |H(rR, k)|^2 \phi_X(rR, k)}, \quad (104)$$

and the broadband MSE is defined as

$$\begin{aligned} J(H) &= \sum_{r,k} J[H(rR, k)] \\ &= \sum_{r,k} |1 - H(rR, k)|^2 \phi_X(rR, k) + \sum_{r,k} |H(rR, k)|^2 \phi_V(rR, k). \end{aligned} \quad (105)$$

## Example 5

Consider a speech signal,  $x(t)$ , sampled at 16 kHz, that is corrupted with uncorrelated additive white Gaussian noise,  $v(t) \sim \mathcal{N}(0, \sigma_v^2)$ . The observed signal,  $y(t)$ , given by  $y(t) = x(t) + v(t)$ , is transformed into the STFT domain, multiplied at each time-frequency bin with a spectral gain  $H(rR, k)$ , and transformed back into the time domain by using (91) and (92).

To demonstrate noise reduction in the STFT domain, we choose a Hamming window of length  $L = 512$  as the analysis window, a decimation factor  $R = L/4 = 128$ , and the Wiener gain in the STFT domain:

$$H_W(rR, k) = \frac{i\text{SNR}(rR, k)}{1 + i\text{SNR}(rR, k)}. \quad (106)$$

An estimate for the noise variance  $\hat{\phi}_V(rR, k)$  can be simply obtained by averaging past spectral power values of the noisy measurement during speech inactivity:

$$\hat{\phi}_V(rR, k) = \begin{cases} \alpha \hat{\phi}_V[(r-1)R, k] + (1-\alpha) |Y(rR, k)|^2, & X(rR, k) = 0 \\ \hat{\phi}_V[(r-1)R, k], & X(rR, k) \neq 0 \end{cases}, \quad (107)$$

where  $\alpha$  ( $0 < \alpha < 1$ ) denotes a smoothing parameter.

This method requires a voice activity detector (VAD), but there are also alternative and more efficient methods that are based on minimum statistics [19], [20].

Finding an estimate for  $\phi_X(rR, k)$  is a much more challenging problem [21], [22].

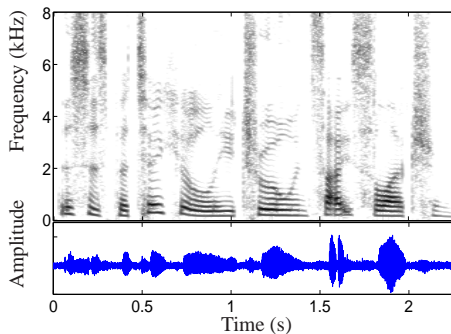
In this example, for simplicity, we smooth  $|Y(rR, k)|^2$  in both time and frequency axes and subtract an estimate of the noise that is multiplied with an oversubtraction factor  $\beta$  ( $\beta \geq 1$ ), i.e.,

$$\hat{\phi}_X(rR, k) = \max \left\{ \hat{\phi}_Y(rR, k) - \beta \hat{\phi}_V(rR, k), 0 \right\}, \quad (108)$$

where  $\hat{\phi}_Y(rR, k)$  is obtained as a two-dimensional convolution between  $|Y(rR, k)|^2$  and a smoothing window  $w(rR, k)$ .

Here, the smoothing window is a two-dimensional Hamming window of size  $3 \times 11$ , normalized to  $\sum_{r,k} w(rR, k) = 1$ .

Figure 13 shows the spectrogram (magnitude of the STFT representation) and waveform of the clean speech signal,  $x(t)$ .



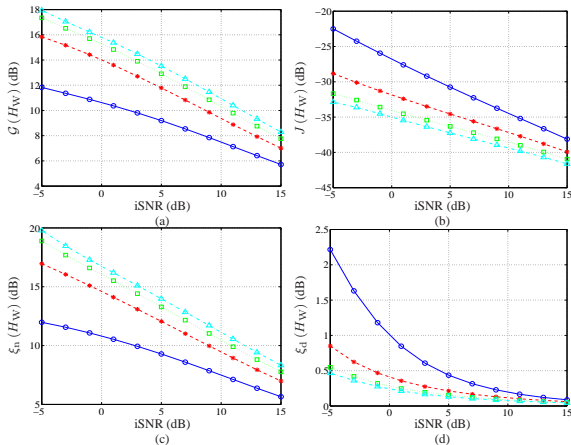
**Figure 13:** Speech spectrogram and waveform of a clean speech signal,  $x(t)$ : “This is particularly true in site selection.”

Figure 14 shows plots of the broadband gain in SNR, the broadband MSE,  $J(H_W)$ , the broadband noise reduction factor,  $\xi_n(H_W)$ , and the broadband desired-signal reduction factor,  $\xi_d(H_W)$ , as a function of the broadband input SNR for different values of the oversubtraction factor  $\beta$ .

Figure 15 shows a realization of the noise corrupted and filtered speech signals for different values of  $\beta$ .

For larger values of  $\beta$ , there is less residual musical noise, but at the expense of larger distortion of weak speech components.

Note that more useful algorithms for enhancing noisy speech signals in the STFT domain are presented in [1], [23], [24].



**Figure 14:** The broadband (a) gain in SNR, (b) MSE, (c) noise reduction factor, and (d) desired-signal reduction factor of the Wiener gain for different oversubtraction factors  $\beta$ :  $\beta = 1$  (solid line with circles),  $\beta = 2$  (dashed line with asterisks),  $\beta = 3$  (dotted line with squares), and  $\beta = 4$  (dash-dot line with triangles).

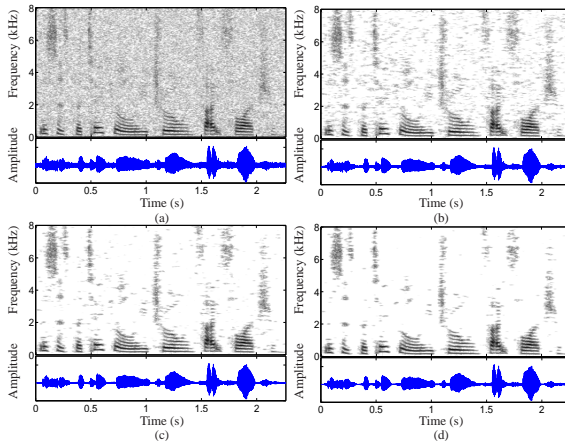


**Figure 15:** Speech spectrograms and waveforms of (a) noisy speech signal,  $y(t)$ , (b) filtered signal,  $z(t)$ , using an oversubtraction factor,  $\beta = 1$ , (c) filtered signal,  $z(t)$ , using an oversubtraction factor,  $\beta = 2$ , and (d) filtered signal,  $z(t)$ , using an oversubtraction factor,  $\beta = 3$ .

- [1] J. Benesty, J. Chen, Y. Huang, and I. Cohen, *Noise Reduction in Speech Processing*. Berlin, Germany: Springer-Verlag, 2009.
- [2] W. Etter and G. S. Moschytz, "Noise reduction by noise-adaptive spectral magnitude expansion," *J. Audio Eng. Soc.*, vol. 42, pp. 341–349, May 1994.
- [3] J. S. Lim and A. V. Oppenheim, "Enhancement and bandwidth compression of noisy speech," *Proc. IEEE*, vol. 67, pp. 1586–1604, Dec. 1979.
- [4] Y. Ephraim and D. Malah, "Speech enhancement using a minimum mean-square error short-time spectral amplitude estimator," *IEEE Trans. Acoust., Speech, Signal Process.*, vol. ASSP-32, pp. 1109–1121, Dec. 1984.
- [5] R. J. McAulay and M. L. Malpass, "Speech enhancement using a soft-decision noise suppression filter," *IEEE Trans. Acoust., Speech, Signal Process.*, vol. ASSP-28, pp. 137–145, Apr. 1980.
- [6] M. M. Sondhi, C. E. Schmidt, and L. R. Rabiner, "Improving the quality of a noisy speech signal," *Bell Syst. Techn. J.*, vol. 60, pp. 1847–1859, Oct. 1981.
- [7] M. Berouti, R. Schwartz, and J. Makhoul, "Enhancement of speech corrupted by acoustic noise," in *Proc. IEEE ICASSP*, 1979, pp. 208–211.

- [8] S. F. Boll, "Suppression of acoustic noise in speech using spectral subtraction," *IEEE Trans. Acoust., Speech, Signal Process.*, vol. ASSP-27, pp. 113–120, Apr. 1979.
- [9] M. R. Schroeder, "Apparatus for suppressing noise and distortion in communication signals," U.S. Patent No. 3,180,936, filed Dec. 1, 1960, issued Apr. 27, 1965.
- [10] M. R. Schroeder, "Processing of communication signals to reduce effects of noise," U.S. Patent No. 3,403,224, filed May 28, 1965, issued Sept. 24, 1968.
- [11] M. R. Weiss, E. Aschkenasy, and T. W. Parsons, "Processing speech signals to attenuate interference," in *Proc. IEEE Symposium on Speech Recognition*, 1974, pp. 292–295.
- [12] E. J. Diethorn, "Subband noise reduction methods for speech enhancement," in *Audio Signal Processing for Next-Generation Multimedia Communication Systems*, Y. Huang and J. Benesty, Eds., Boston, MA, USA: Kluwer, 2004, Chapter 4, pp. 91–115.
- [13] J. H. L. Hansen, "Speech enhancement employing adaptive boundary detection and morphological based spectral constraints," in *Proc. IEEE ICASSP*, 1991, pp. 901–904.

- [14] Y. Lu and P. C. Loizou, "A geometric approach to spectral subtraction," *Speech Communication*, vol. 50, pp. 453–466, 2008.
- [15] B. L. Sim, Y. C. Tong, J. S. Chang, and C. T. Tan, "A parametric formulation of the generalized spectral subtraction method," *IEEE Trans. Speech, Audio Process.*, vol. 6, pp. 328–337, July 1998.
- [16] J. Wexler and S. Raz, "Discrete Gabor expansions," *Speech Process.*, vol. 21, pp. 207–220, Nov. 1990.
- [17] S. Qian and D. Chen, "Discrete Gabor transform," *IEEE Trans. Signal Process.*, vol. 41, pp. 2429–2438, July 1993.
- [18] R. E. Crochiere and L. R. Rabiner, *Multirate Digital Signal Processing*. Englewood Cliffs, New Jersey: Prentice-Hall, 1983.
- [19] R. Martin, "Noise power spectral density estimation based on optimal smoothing and minimum statistics," *IEEE Trans. Speech and Audio Process.*, vol. 9, pp. 504–512, July 2001.
- [20] I. Cohen, "Noise spectrum estimation in adverse environments: improved minima controlled recursive averaging," *IEEE Trans. Speech and Audio Process.*, vol. 11, pp. 466–475, Sept. 2003.

- [21] I. Cohen, “Relaxed statistical model for speech enhancement and a priori SNR estimation,” *IEEE Trans. Speech and Audio Process.*, vol. 13, pp. 870–881, Sept. 2005.
- [22] I. Cohen, “Speech spectral modeling and enhancement based on autoregressive conditional heteroscedasticity models,” *Signal Process.*, vol. 86, pp. 698–709, Apr. 2006.
- [23] I. Cohen and B. Berdugo, “Speech enhancement for non-stationary noise environments,” *Signal Process.*, vol. 81, pp. 2403–2418, Nov. 2001.
- [24] I. Cohen and S. Gannot, “Spectral Enhancement Methods,” in J. Benesty, M. Mohan Sondhi and Y. Huang (Eds.), *Springer Handbook of Speech Processing*, Springer, 2008, Part H, Ch. 44, pp. 873–901.